

A gas-filled recoil separator, SHANS



Z.Y. Zhang^a, L. Ma^{a,b,c}, Z.G. Gan^{a,*}, M.H. Huang^a, T.H. Huang^a, G.S. Li^a, X.L. Wu^a, G.B. Jia^{a,b,1}, L. Yu^{a,b}, H.B. Yang^{a,b}, Z.Y. Sun^a, X.H. Zhou^a, H.S. Xu^a, W.L. Zhan^a

^a Institute of Modern Physics, Chinese Academy of Sciences, Lanzhou 730000, China

^b University of Chinese Academy of Sciences, Beijing 100049, China

^c School of Nuclear Science and Technology, Lanzhou University, Lanzhou 730000, China

ARTICLE INFO

Article history:

Received 13 March 2013

Received in revised form 23 May 2013

Accepted 29 May 2013

Available online 19 June 2013

Keywords:

Gas-filled recoil separator

Heavy nuclei

Fusion reaction products

ABSTRACT

A gas-filled recoil separator, SHANS (Spectrometer for Heavy Atom and Nuclear Structure), constructed at the Institute of Modern Physics in Lanzhou is reported. With the QDQQ magnetic configuration, where *D* and *Q* denote the dipole and quadrupole magnets respectively, the apparatus is used to study the heavy nuclei produced in the heavy-ion-induced fusion reactions. The helium gas is filled in the field region of the separator at a pressure of about 1 mbar. The maximum magnetic rigidity of the dipole magnet is 2.9 Tm. With the commissioning of the device, the performance of the separator in several fusion evaporation reactions is investigated.

© 2013 Elsevier B.V. All rights reserved.

1. Introduction

For the last half century, the kinematic recoil separator has been an useful tool to separate and study the heavy nuclei produced in complete fusion reactions (see, e.g., Refs. [1–3]). In the device, the fusion evaporation products recoiling out of a thin target can be efficiently separated in-flight from the primary beam particles and other unwanted products. The separation time is extremely short on the order of 1 μs. The gas-filled recoil separator [4,5] is one type of the most successful separation instruments. It was originally developed for the separation of fission products to study the charge distribution of fragments [6]. Later on, the separation method was used in studies of evaporation residues (EVRs) of complete fusion-reaction products.

Currently, with the application of this type of device, the heaviest elements with atomic number $Z = 113$ – 118 are firstly studied in $^{209}\text{Bi} (^{70}\text{Zn}, n)^{278}113$ reaction [7–9] and ^{48}Ca -induced hot-fusion reactions [2]. The detailed spectroscopy in the actinide and transactinide nuclei region [10,11] and the cold fusion reactions for odd- Z projectiles with ^{208}Pb target [12,13] are investigated systematically. Furthermore, as a pre-separator, the device is also used for the heavy-element chemistry experiments [14,15]. Several similar gas-filled recoil separators are now in use, which are DGFERS at JINR [16], BGS at LBNL [17], TASCA at GSI [18], RITU at JYFL [19], and GARIS at RIKEN [20], and so on.

To study the heavy and superheavy nuclei properties, a gas-filled recoil separator, SHANS (Spectrometer for Heavy Atom and Nuclear Structure), was constructed recently at the Institute of Modern Physics (IMP), in Lanzhou, China. In this paper, we describe the configuration and technical parameters of the separator in detail. The primary experimental performance of the device in the $^{40}\text{Ar} + ^{175}\text{Lu}$, $^{64}\text{Ni} + ^{208}\text{Pb}$ and $^{40}\text{Ca} + ^{175}\text{Lu}$ reactions is also discussed.

2. Spectrometer

2.1. Operation principle

For the synthesis and studies of heavy nuclei, the heavy-ion-induced fusion reactions are normally used. When the EVRs recoiling from a thin target move in dilute gas and experience a large number of collisions with the gas molecules, their charge states will fluctuate around an average charge state (q_{ave}) resulting from electron capture and loss processes [21]. Then the motion of the interest ions in a gas-filled dipole magnetic field is determined by the following equation,

$$B\rho = mv/q_{ave}e, \quad (1)$$

where B is the magnetic flux density, ρ is the curvature radius of the trajectory for the particles, e is the elementary charge, m and v are the mass and velocity of the ions, respectively. According to Bohr's assumption [22], for a nuclear species Z^A , the expression for average charge state

$$q_{ave} = (v/v_0) \cdot Z^{1/3} \quad (2)$$

* Corresponding author. Tel.: +86 931 4969304.

E-mail address: zggan@impcas.ac.cn (Z.G. Gan).

¹ Present address: Shanghai Institute of Applied Physics, Chinese Academy of Sciences, Shanghai 201800, China.

is obtained from the atomic Thomas–Fermi model in the first order approximation within a velocity range $1 < v/v_0 < Z^{2/3}$, where v_0 is the Bohr velocity (2.19×10^6 m/s). Thus, the magnetic rigidity $B\rho$ can be expressed as the formula,

$$B\rho = 0.02267 \cdot A/Z^{1/3} (\text{Tm}), \quad (3)$$

which is approximately proportional to $Z^{2/3}$. It is indicated that the $B\rho$ is independent of the initial charge state distribution and the velocity of the particles. The corresponding trajectories of the ions are only determined by the mass and atomic number. Consequently, the EVRs can be efficiently separated in-flight from unreacted beam and other transfer products by their largest magnetic rigidity. The main loss of EVRs is due to the ion optical characteristics and scattering with gas molecules. However, in most cases, formula (2) overestimates q_{ave} . The fact that the average charge state is related to v, Z , the type and pressure of the filling gas is clearly shown in Ref. [5,25]. The accurate estimation of the q_{ave} is necessary for setting the proper magnetic rigidity. In general, due to the lack of knowledge about charge exchange cross-sections, the average charge state q_{ave} can only be calculated by some semi-empirical expressions [5,23–25].

2.2. Status of the gas-filled recoil separator, SHANS

The schematic view of the gas-filled recoil separator, SHANS, is shown in Fig. 1. The separator consists of four magnets in a $Q_v D_h Q_v Q_h$ configuration, where D refers to a dipole magnet and Q to a quadrupole magnet, as well as the subscripts h and v stand for horizontally and vertically focusing, respectively. Comparison with the classical DQQ configuration, an additional quadrupole magnet with vertically focusing direction is added in front of the dipole for matching with the dipole acceptance and increasing the angular acceptance (25 msr). The dipole magnet is designed with a horizontally focusing quadrupole component aimed to obtain high transport efficiency. The 52° bending angle of dipole is beneficial to reduce the background particles scattered onto the focal plane. The large maximum magnetic rigidity (2.9 Tm) of dipole magnet is suitable to separate the heavy and superheavy nuclei produced in cold and hot fusion reactions. Some of the characteristics of each magnet are shown in Table 1.

Pure helium gas at about 1 mbar pressure is filled in the separator to achieve the required charge state exchange statistics. A differential pumping system is installed upstream of the target to isolate the vacuum region of accelerator side and the gas-filled

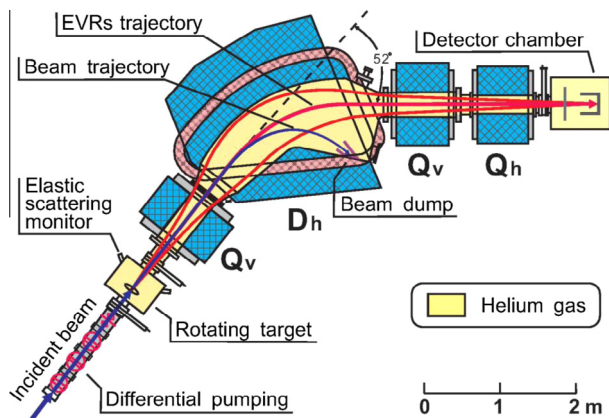


Fig. 1. A schematic view of the gas-filled recoil separator, SHANS. D_h denotes the dipole magnet with horizontally focusing ability. Q_v and Q_h stand for vertically and horizontally focusing quadrupole magnets, respectively. The typical trajectories of primary beam and evaporation residues are also indicated.

Table 1
Technical parameters of the gas-filled separator.

Parameters	Values
Configuration	$Q_v D_h Q_v Q_h$
Total length	6.5 m
Angular acceptance	25 msr
Dispersion	7.3 mm/% $B\rho$
<i>D_h magnet</i>	
Bending radius	1.8 m
Central trajectory length	1.6 m
Bending angle	52°
Maximum magnetic rigidity	2.9 Tm
Entrance angle	-45°
Exit angle	22°
<i>Q_v magnets</i>	
Effective length	667 mm
Aperture radius	120 mm
Maximum field gradient	6.8 T/m
<i>Q_h magnet</i>	
Effective length	500 mm
Aperture radius	85 mm
Maximum field gradient	8.9 T/m

region leading to window-less operation. Using this pumping system, the pressure at the accelerator side could keep about 7 orders lower than the target chamber. In order to tolerate a very intense heavy ion beam, a rotating target system is installed at the target position for preparing the experiments with low melting point targets. The maximum rotating speed of the wheel is up to 2000 rpm. A beam chopper is used to avoid irradiating the target frame. And the chopping signal is recorded by the data acquisition system in order to distinguish between beam-on events and beam-off ones. In experiment, the beam intensity is monitored by four silicon avalanche photodiodes (APD) to measure beam particles elastically scattered by the target nuclei. They are mounted at $\pm 30^\circ$ and $\pm 45^\circ$ with respect to the incident beam direction. The unreacted incident beam is stopped by a copper box installed inside the dipole chamber.

A silicon semiconductor detector box (Si-box) is installed at the focal plane position of the separator. Three 300- μm thick Position Sensitive Silicon Detectors (PSSD) are mounted at the back of Si-box as implantation detectors. They have total active area of $150 \times 50 \text{ mm}^2$ and are divided into 48 independent vertical strips

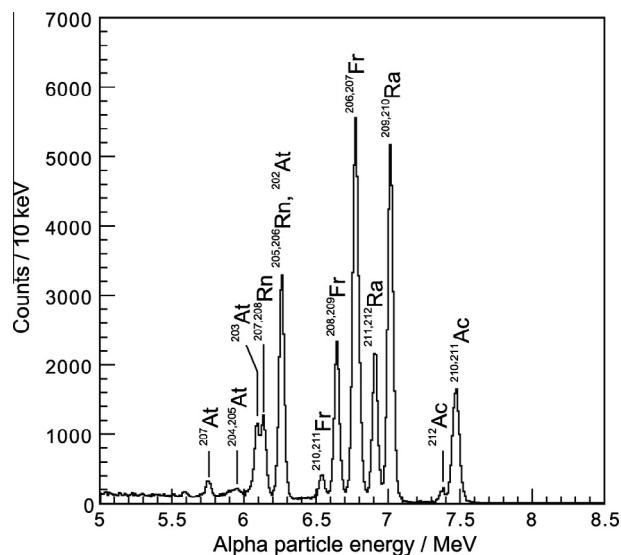


Fig. 2. α -Particle energy spectrum measured in the silicon strip detectors and vetoed with the MWPC using the 204 MeV $^{40}\text{Ca}+^{175}\text{Lu}$ reaction.

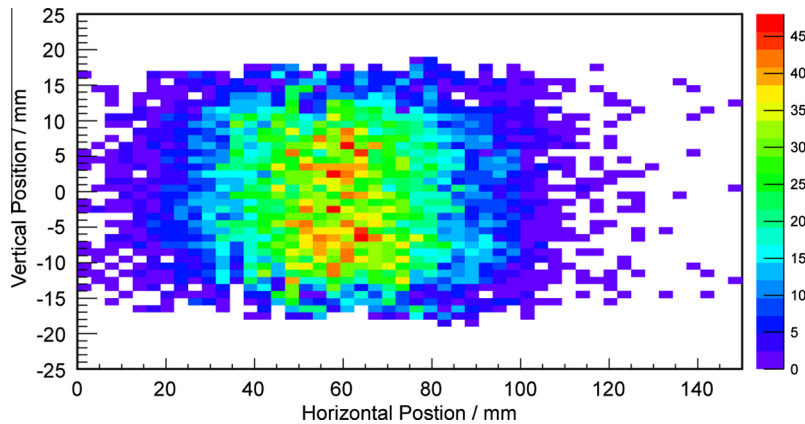


Fig. 3. The position distribution of the decay of $^{210,211}\text{Ac}$ obtained with the implantation detectors at 0.8-mbar pressure of He and the 1.72-Tm magnetic rigidity. The image is projected onto the area of $150 \times 50 \text{ mm}^2$.

providing 3-mm horizontal position accuracy. Signals are provided from both the top and bottom of each strip. Resistive charge division provides 1.5-mm vertical position resolution with each strip. The typical energy resolution of PSSD is 50 keV FWHM for 5–10 MeV α particles. Signals from the preamplifiers are processed through two amplification branches, one for measuring 1–20 MeV α particles and the other for measuring implantation and fission fragments with energies of 5–200 MeV. Eight non-position-sensitive silicon detectors are mounted in an open box arrangement around the strip detectors. They are used to detect the escaping radioactive decay events. Three punch-through detectors, which have the same size and thickness as the implantation detectors, are mounted behind the PSSD to provide veto signals for light particles passing through the strip detectors.

A Multi-Wire Proportional Counter (MWPC) is mounted upstream of the Si-box as a timing detector, which have an active area of $180 \times 80 \text{ mm}^2$. When arriving the detector chamber, the recoils pass through the MWPC and are finally implanted into the PSSD. The time-of-flight measurement allows us to distinguish the radioactive decay events in the PSSD from the implantation ones. The events without signals from the timing detector are regarded as the decay events. The event chains consisting of implanted EVRs and their subsequent α decay and/or spontaneous fission are identified by the position-and-time correlation method [1].

3. Performance of the separator

In the first testing experiment, the complete fusion reaction, $^{175}\text{Lu} (^{40}\text{Ar}, 4-5n)^{210,211}\text{Ac}$, was performed on the gas-filled separator to study the basic separation performance. The stationary target was used. Only one position-sensitive PIPS detector with an active area of $58 \times 58 \text{ mm}^2$ was mounted at the focal plane position. The measurement of magnetic rigidity distribution at different helium gas pressures showed that the optimum pressure was in the range of 0.8–1.0 mbar with the minimum of the image size. The measured transport efficiency for 4–5n reaction products was 14%. However, this value should be considered a lower limit due to the 50% uncertainty of the reference cross section [26] and the insufficient detector active area.

As the first superheavy nuclei experiment on the device, the cold fusion reaction, $^{208}\text{Pb} (^{64}\text{Ni}, n)^{271}\text{Ds}$, was carried out at a beam energy of 317 MeV. The total counting rate in the focal plane detector was about 25 s^{-1} at the beam intensity of 6.6×10^{11} ions/s. And the rate of the 7–11 MeV α -particle energy region was 3.5 s^{-1} . In the experiment, one correlated α -decay chain assigned to the decay of ^{271}Ds nucleus was observed. The implantation event with

the energy of 30.63 MeV was followed by three α particles with 7–11 MeV energy in the same position window. The observed 10.644-MeV α -particle decay energy and 96.8-ms decay time for the ^{271}Ds are consistent with the values reported in the Ref. [12,27,28]. The details of the decay chain are discussed in Ref. [29].

Recently, with the newly installed detection system (MWPC + Si-box), a measurement was made using a ^{40}Ca beam at 204 MeV incident on a stationary $500\text{-}\mu\text{g}/\text{cm}^2$ thick ^{175}Lu target. The target was evaporated on a carbon backing ($33\text{-}\mu\text{g}/\text{cm}^2$ thickness). The MWPC-vetoed α -particle energy spectrum obtained by the strip detectors is shown in Fig. 2. Several isotopes from xpyv evaporation channels and their subsequent α -decay nuclei were identified by their decay energies. The suppression of the full energy primary beam was estimated to be a factor of 10^{15} . Fig. 3 shows the position spectrum of the decay of $^{210,211}\text{Ac}$ at the implantation detectors under the condition of 0.8-mbar pressure of Helium gas and the 1.72-Tm magnetic rigidity. With a dispersion of $7.3 \text{ mm}/\%B\rho$, an acceptance interval ($\Delta B\rho$) of $\pm 0.11 \text{ Tm}$ ($\pm 6\%$) is defined by the horizontal position distribution of the isotopes $^{210,211}\text{Ac}$.

4. Conclusion

A gas-filled recoil separator, SHANS, with the type of $Q_v D_h Q_v Q_h$ configuration is commissioned at IMP, which is dedicated to the studies of heavy nuclei produced in heavy-ion-induced fusion reactions. The large angular acceptance, bending angle and maximum magnetic rigidity are designed. The complete fusion reactions, $^{40}\text{Ar} + ^{175}\text{Lu}$, $^{64}\text{Ni} + ^{208}\text{Pb}$ and $^{40}\text{Ca} + ^{175}\text{Lu}$, were performed on the separator and the fusion evaporation products were observed clearly by the focal plane detection system. For the future work, the research activity will be mainly concentrated on the study of the very neutron-deficient isotopes in the actinide or transactinide region.

Acknowledgements

The authors thank greatly all accelerator staff for providing intense and stable beams. We also would like to thank the members from GSI SHIP group and RIKEN GARIS group for useful discussions and suggestions. This work is supported by the National Basic Research Program of China (No. 2013CB834403), the National Natural Science Fund for Distinguished Young Scholars (No. 10925526), the Project of International Cooperation and Exchanges (NSFC No. 11120101005) and the National Natural Science Foundation of China (No. 11005128).

References

- [1] S. Hofmann, G. Münzenberg, *Rev. Mod. Phys.* 72 (2000) 733.
- [2] Y. Oganessian, *J. Phys. G* 34 (2007) R165.
- [3] C.E. Düllmann, *Nucl. Instr. Meth. B* 266 (2008) 4123.
- [4] M. Leino, *Nucl. Instr. Meth. B* 204 (2003) 129.
- [5] A. Ghiorso, S. Yashita, M.E. Leino, L. Frank, J. Kalnins, P. Armbruster, J.P. Dufour, P.K. Lemmert, *Nucl. Instr. Meth. A* 269 (1988) 192.
- [6] B.L. Cohen, C.B. Fulmer, *Nucl. Phys.* 6 (1958) 547.
- [7] K. Morita, K. Morimoto, D. Kaji, T. Akiyama, S. Goto, H. Haba, E. Ideguchi, R. Kanungo, K. Katori, H. Koura, H. Kudo, T. Ohnishi, A. Ozawa, T. Suda, K. Sueki, H.S. Xu, T. Yamaguchi, A. Yoneda, A. Yoshida, Y.L. Zhao, *J. Phys. Soc. Jpn.* 73 (2004) 2593.
- [8] K. Morita, K. Morimoto, D. Kaji, T. Akiyama, S. Goto, H. Haba, E. Ideguchi, K. Katori, H. Koura, H. Kikunaga, H. Kudo, T. Ohnishi, A. Ozawa, N. Sato, T. Suda, K. Sueki, F. Tokanai, T. Yamaguchi, A. Yoneda, A. Yoshida, *J. Phys. Soc. Jpn.* 76 (2007) 2.
- [9] K. Morita, K. Morimoto, D. Kaji, H. Haba, K. Ozeki, Y. Kudou, T. Sumita, Y. Wakabayashi, A. Yoneda, K. Tanaka, *J. Phys. Soc. Jpn.* 81 (2012) 103201.
- [10] R.D. Herzberg, P.T. Greenlees, *Prog. Part. Nucl. Phys.* 61 (2008) 674.
- [11] R.D. Herzberg, D.M. Cox, *Radiochim. Acta* 99 (2011) 441.
- [12] C.M. Folden, K.E. Gregorich, C.E. Düllmann, H. Mahmud, G.K. Pang, J.M. Schwantes, R. Sudowe, P.M. Zielinski, H. Nitsche, D.C. Hoffman, *Phys. Rev. Lett.* 93 (2004) 212702.
- [13] C.M. Folden, S.L. Nelson, C.E. Düllmann, J.M. Schwantes, R. Sudowe, P.M. Zielinski, K.E. Gregorich, H. Nitsche, D.C. Hoffman, *Phys. Rev. C* 73 (2006) 014611.
- [14] C.E. Düllmann, C.M. Folden, K.E. Gregorich, D.C. Hoffman, D. Leitner, G.K. Pang, R. Sudowe, P.M. Zielinski, H. Nitsche, *Nucl. Instr. Meth. A* 551 (2005) 528.
- [15] H. Haba, T. Akiyama, D. Kaji, H. Kikunaga, T. Kuribayashi, K. Morimoto, K. Morita, K. Ooe, N. Sato, A. Shinohara, T. Takabe, Y. Tashiro, A. Toyoshima, A. Yoneda, T. Yoshimura, *Eur. Phys. J. D* 45 (2007) 81.
- [16] K. Subotic, Y.T. Oganessian, V.K. Utyonkov, Y.V. Lobanov, F.S. Abdullin, A.N. Polyakov, Y.S. Tsyganov, O.V. Ivanov, *Nucl. Instr. Meth. A* 481 (2002) 71.
- [17] V. Ninov, K.E. Gregorich, T.N. Ginter, F.P. Heberger, R. Krücken, D.M. Lee, W. Loveland, W.D. Myers, J. Patin, M.W. Rowe, N.K. Seward, W.J. Swiatecki, A. Türler, P.A. Wilk, *Nucl. Phys. A* 682 (2001) 98c.
- [18] A. Semchenkov, W. Bröchle, E. Jäger, E. Schimpf, M. Schädel, C. Mühle, F. Klos, A. Türler, A. Yakushev, A. Belov, T. Belyakova, M. Kaparkova, V. Kukhtin, E. Lamzin, S. Sytchevsky, *Nucl. Phys. B* 266 (2008) 4153.
- [19] M. Leino, J. Äystö, T. Enqvist, P. Heikkinen, A. Jokinen, M. Nurmi, A. Ostrowski, W.H. Trzaska, J. Uusitalo, K. Eskola, P. Armbruster, V. Ninov, *Nucl. Instr. Meth. B* 99 (1995) 653.
- [20] K. Morita, A. Yoshida, T.T. Inamura, M. Koizumi, T. Nonura, M. Fujioka, T. Shinozuka, H. Miyatake, K. Sueki, H. Kudo, Y. Nagai, T. Toriyama, K. Yoshimura, Y. Hatsukawa, *Nucl. Instr. Meth. B* 70 (1992) 220.
- [21] H.D. Betz, *Rev. Mod. Phys.* 44 (1972) 465.
- [22] N. Bohr, *Phys. Rev.* 58 (1940) 654.
- [23] K.E. Gregorich, W. Loveland, D. Peterson, P.M. Zielinski, S.L. Nelson, Y.H. Chung, C.E. Düllmann, C.M. Folden, K. Aleklett, R. Eichler, D.C. Hoffman, J.P. Omtvedt, G.K. Pang, J.M. Schwantes, S. Sovrana, P. Sprunger, R. Sudowe, R.E. Wilson, H. Nitsche, *Phys. Rev. C* 72 (2005) 014605.
- [24] Y.T. Oganessian, Y.V. Lobanov, A.G. Popeko, F.S. Abdullin, Y.P. Kharitonov, A.A. Ledovskoy, Y.S. Tsyganov, *Z. Phys. Z. Phys. D* 21 (1991) S357.
- [25] J. Khuyagbaatar, D. Ackermann, L.L. Andersson, J. Ballof, W. Bröchle, C.E. Düllmann, J. Dvorak, K. Eberhardt, J. Even, A. Gorshkov, R. Graeger, F.P. Heberger, D. Hild, R. Hoischen, E. Jäger, B. Kindler, J.V. Kratz, S. Lahiri, B. Lommel, M. Maiti, E. Merchan, D. Rudolph, M. Schädel, H. Schaffner, B. Schausten, E. Schimpf, A. Semchenkov, A. Serov, A. Türler, A. Yakushev, *Nucl. Instr. Meth. A* 689 (2012) 40.
- [26] D. Vermeulen, H.-G. Clerc, C.-C. Sahn, K.-H. Schmidt, J.G. Keller, G. Münzenberg, W. Reisdorf, *Z. Phys. A* 318 (1984) 157.
- [27] K. Morita, K. Morimoto, D. Kaji, H. Haba, E. Ideguchi, R. Kanungo, K. Katori, H. Koura, H. Kudo, T. Ohnishi, A. Ozawa, T. Suda, K. Sueki, I. Tanihata, H. Xu, A.V. Yeremin, A. Yoneda, A. Yoshida, Y.L. Zhao, T. Zheng, *Eur. Phys. J. A* 21 (2004) 257.
- [28] S. Hofmann, *Rep. Prog. Phys.* 61 (1998) 639.
- [29] Z.Y. Zhang, Z.G. Gan, L. Ma, M.H. Huang, T.H. Huang, X.L. Wu, G.B. Jia, G.S. Li, L. Yu, Z.Z. Ren, S.G. Zhou, Y.H. Zhang, X.H. Zhou, H.S. Xu, H.Q. Zhang, G.Q. Xiao, W.L. Zhan, *Chin. Phys. Lett.* 29 (2012) 012502.